

3. Sailer A, Dichgans J, Gerloff C. The influence of normal aging on the cortical processing of a simple motor task. *Neurology* 2000;55:979–985.
4. Agnati LF, Zoli M, Grimaldi R, et al. Cellular and synaptic alterations in the aging brain. *Aging (Milano)* 1990;2:5–25.
5. Classen J, Liepert J, Wise SP, et al. Rapid plasticity of human cortical movement representation induced by practice. *J Neurophysiol* 1998;79:1117–1123.
6. Butefisch CM, Davis BC, Wise SP, et al. Mechanisms of use-dependent plasticity in the human motor cortex. *Proc Natl Acad Sci USA* 2000;97:3661–3665.
7. Sawaki L, Boroojerdi B, Kaelin-Lang A, et al. Cholinergic influences on use-dependent plasticity. *J Neurophysiol* 2002;87:166–171.
8. Liepert J, Miltner WH, Bauder H, et al. Motor cortex plasticity during constraint-induced movement therapy in stroke patients. *Neurosci Lett* 1998;250:5–8.
9. Reddy H, Narayanan S, Arnoutelis R, et al. Evidence for adaptive functional changes in the cerebral cortex with axonal injury from multiple sclerosis. *Brain* 2000;123:2314–2320.
10. Nudo RJ, Plautz EJ, Frost SB. Role of adaptive plasticity in recovery of function after damage to motor cortex. *Muscle Nerve* 2001;24:1000–1019.
11. Rypma B, D'Esposito M. Isolating the neural mechanisms of age-related changes in human working memory. *Nat Neurosci* 2000;3:509–515.
12. Langley LK, Madden DJ. Functional neuroimaging of memory: implications for cognitive aging. *Microsc Res Tech* 2000;51:75–84.
13. Jouvenceau A, Dutar P, Billard JM. Alteration of NMDA receptor-mediated synaptic responses in CA1 area of the aged rat hippocampus: contribution of GABAergic and cholinergic deficits. *Hippocampus* 1998;8:627–637.
14. Clayton DA, Grosshans DR, Browning MD. Aging and surface expression of hippocampal NMDA receptors. *J Biol Chem* 2002;277:14367–14369.
15. Sattin RW. Falls among older persons: a public health perspective. *Annu Rev Public Health* 1992;13:489–508.
16. Taub E, Uswatte G, Pidikiti R. Constraint-Induced Movement Therapy: a new family of techniques with broad application to physical rehabilitation—a clinical review. *J Rehabil Res Dev* 1999;36:237–251.
17. Donchin O, Sawaki L, Madupu G, et al. Mechanisms influencing acquisition and recall of motor memories. *J Neurophysiol* 2002;88:2114–2123.
18. Teasdale N, Simoneau M. Attentional demands for postural control: the effects of aging and sensory reintegration. *Gait Posture* 2001;14:203–210.
19. Small GW, La Rue A, Komo S, et al. Predictors of cognitive change in middle-aged and older adults with memory loss. *Am J Psychiatry* 1995;152:1757–1764.
20. Smith MJ, Keel JC, Greenberg BD, et al. Menstrual cycle effects on cortical excitability. *Neurology* 1999;53:2069–2072.

Continuous Growth of Mean Tumor Diameter in a Subset of Grade II Gliomas

Emmanuel Mandonnet, PhD,^{1–5} Jean-Yves Delattre, MD,¹ Marie-Laure Tanguy, MSc,² Kristin R. Swanson, PhD,^{3,4} Antoine F. Carpentier, MD, PhD,¹ Hugues Duffau, MD, PhD,⁵ Philippe Cornu, MD,⁵ Rémy Van Effenterre, MD,⁵ Ellsworth C. Alvord, Jr., MD,³ and Laurent Capelle, MD⁵

Serial magnetic resonance images of 27 patients with untreated World Health Organization grade II oligodendrogliomas or mixed gliomas were reviewed retrospectively to study the kinetics of tumor growth before anaplastic transformation. Analysis of the mean tumor diameters over time showed constant growth. Linear regression, using a mixed model, found an average slope of 4.1mm per year (95% confidence interval, 3.8–4.4mm/year). Untreated low-grade oligodendrogliomas or mixed gliomas grow continuously during their premalignant phase, and their pattern of growth can be predicted within a relatively narrow range. These findings could be of interest to optimize patients management and follow-up.

Ann Neurol 2003;53:524–528

Although it is well recognized that the fate of most low-grade gliomas is to progress to a higher grade of malignancy,¹ very little is known about their radiological history and growth rates during the “pre-malignant” phase. Do these tumors stabilize, grow irregularly, or grow continuously according to some common law?

To define these issues better, we undertook a study of the evolution of untreated low-grade gliomas before anaplastic transformation.

Patients and Methods

Eligibility Criteria

Magnetic resonance images (MRIs) of consecutive unselected patients followed up at the Salpêtrière Hospital between

From the ¹Fédération de Neurologie Mazarin and INSERM U495, Hôpital de la Salpêtrière (AP-HP), Paris; ²INSERM U472, Hôpital Paul Brousse, Villejuif, France; ³Departments of Pathology and ⁴Laboratory of Neuropathology, University of Washington, Seattle, WA; ⁵Service de Neurochirurgie, Hôpital de la Salpêtrière, Paris, France.

Received Sep 4, 2002, and in revised form Dec 5. Accepted for publication Dec 17, 2002.

Address correspondence to Dr Delattre, Department of Neurology Mazarin, Groupe Hospitalier Pitié-Salpêtrière, 47 Boulevard de l'Hôpital, 75651 Paris Cedex 13, France. E-mail: jean-yves.delattre@psl.ap-hop-paris.fr

1989 and 2001 for a low-grade glioma were retrospectively reviewed. The following inclusion criteria were required: (1) histological proof of supratentorial hemispheric World Health Organization (WHO) grade II glioma (astrocytoma, oligodendroglioma, mixed glioma); (2) absence of specific treatment of the tumor (resection, radiotherapy, or chemotherapy), except for stereotactic biopsy necessary for histological diagnosis; and (3) a minimal follow-up duration of 2 years with at least three consecutive MRIs during the study interval.

Patients left the study when specific treatment was required because of progressive symptoms or malignant transformation (proved by a second biopsy or suspected when contrast enhancement appeared on imaging).

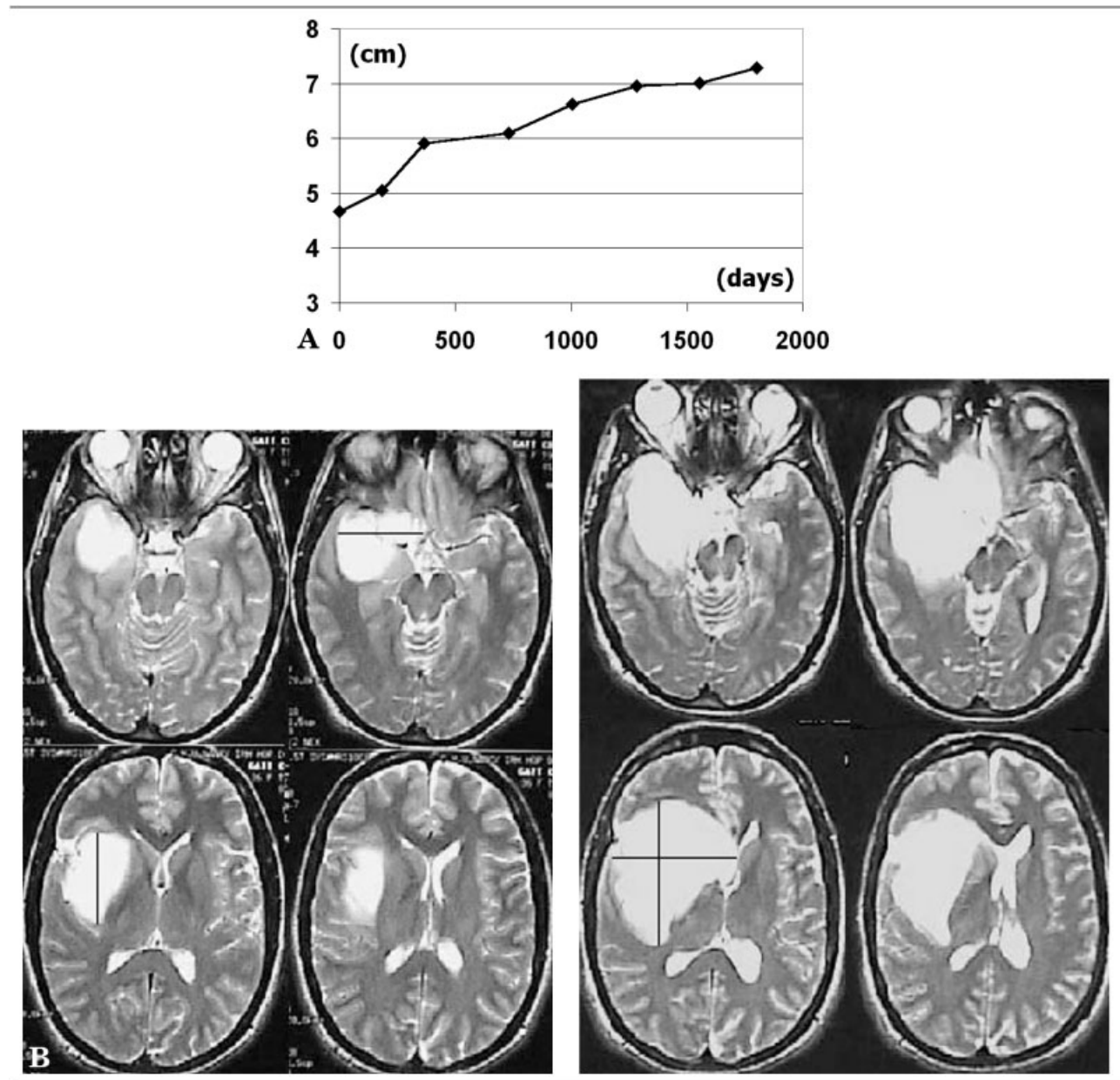
Tumor Diameter Estimation

A recently developed mathematical model of evolution of gliomas,^{2,3} taking into account not only proliferation but also migration/diffusion of tumor cells, predicts a linear growth of mean tumor diameter on MRI. Because linear regression is a simple tool for statistical analysis, the study was focused on the mean tumor diameter, rather than on the surface or the volume of the tumor.

For each MRI, three diameters were manually measured (Fig 1) always by the same neurosurgeon (L.C.) who was blind to patient and examination data and did not participate in the subsequent analysis of the data.

In the axial plane, the largest diameters in the anterior-

Fig 1. Measurement of tumors diameters. (A) Example of the evolution of the mean diameter over time in one patient; (B) corresponding diameters in the axial plane, D1 and D2, on T2-weighted magnetic resonance image at diagnosis (left) and after 1,800 days (right).



posterior axis and perpendicular transverse axis were measured on T2-weighted images.

In the sagittal plane, only a T1-weighted image was available and was used to measure the largest diameter along the vertical axis. The mean diameter was obtained as the geometric mean of the three diameters, that is the cube root of their product.

Statistical Analysis

To estimate the average slope of the growth curve of the mean diameter, we performed a linear regression.

However, because patients had various tumor sizes at the time of diagnosis (lead-time bias), a different starting point (intercept) for each patient was allowed, and a linear mixed model was used with random intercept that can be expressed as

$$D_{ij} = \mu + \alpha_i + \beta \times t_{ij} + \varepsilon_{ij}$$

where D_{ij} denotes the mean diameter for Patient i at time of observation j , $\mu + \alpha_i$ is the intercept for the i th patient, β is a fixed effect parameter representing the slope of the diameter evolution, t_{ij} is the time of observation j for the i th patient, and ε_{ij} is the residual term for the i th patient at the j th time.

All analyses were performed with the SAS software (SAS Institute, Cary, NC).

Results

Clinical Data

Twenty-seven patients (12 women and 15 men) fulfilled the eligibility criteria. The median age at onset of symptoms was 33 years (range, 23–58 years) and 35 years at first MRI (range, 23–59 years). The primary tumor location was frontal in 9 cases, parietal in 3 cases, insular in 10 cases, and temporoparietal in 5 cases. Tumors involved the left hemisphere in 13 patients and the right in 14 patients. At the time of radiological diagnosis, 3 patients were asymptomatic, 2 patients suffered from chronic headaches, and 22 patients had seizures. Only two patients had associated slight focal neurological deficits.

Histology

Histological diagnoses included 22 oligodendrogliomas and 5 mixed gliomas (oligoastrocytomas) according to the WHO classification. No astrocytomas met the inclusion criteria.

During the follow-up period, five patients experienced anaplastic transformations (two oligodendrogliomas, and three mixed gliomas), and left the study at a median time from onset of symptoms of 6 years (range, 3.25–16.9 years). In these patients, the data collected from diagnosis until the point of transformation were included in the analysis.

Magnetic Resonance Imaging Follow-up

Overall, 137 full MRI examinations were available. The median number of MR studies per patient was 4 (mean, 5; range, 3–16). The median duration of radiological follow-up was 4.75 years (mean, 4.55; range, 2.0–7.4 years), with a median interval between MR examinations of 336 days (range, 30–1,800 days).

Growth Curves

The evolution of the mean diameter over time for each patient is presented in Figure 2. Three observations can be made. (1) The mean diameter of tumor on the first MRI varies considerably among patients, from 2.1 to 6.7 cm (mean, 4.0 cm; median, 4.1 cm). (2) The mean tumor diameter of these tumors grow inexorably during the follow-up period in a grossly linear fashion. (3) The curves of individual patients appear grossly parallel, suggesting a relative homogeneity of growth rates.

To test this last suggestion, we performed a linear regression of diameter versus time using a mixed model. The average slope of evolution of the mean diameter over time, β , was 0.00113 cm/day ($\sigma = 0.00005$), corresponding to 4.1 mm/year (95% CI, 3.8–4.4 mm/year). To graphically account for the lead-time bias, we plotted each patient's tumor progression curve against the size-adjusted time.

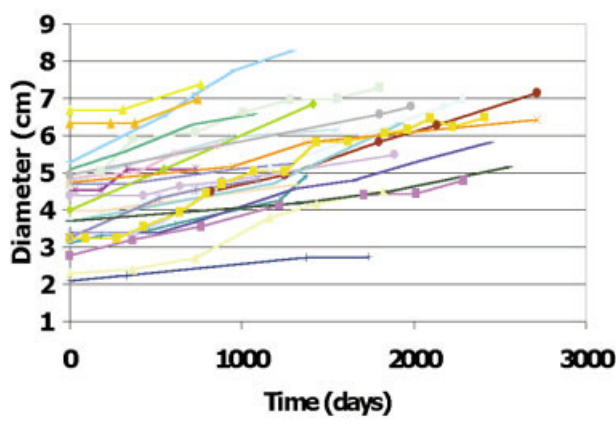
$$t_{ij} = \tau_{ij} + \alpha_i/\beta$$

In this way, all curves are aligned along the common average regression line $D = \mu + \beta t$, and variations from this average behavior are shown in Figure 3.

Discussion

This study indicates that untreated low-grade oligodendrogliomas or mixed gliomas (WHO grade II) grow

Fig 2. Evolution of the mean tumor diameters over time in the 27 patients. Each curve starts at the first magnetic resonance image (MRI) obtained at diagnosis and ends at the last follow-up MRI (or last MRI before anaplastic transformation).



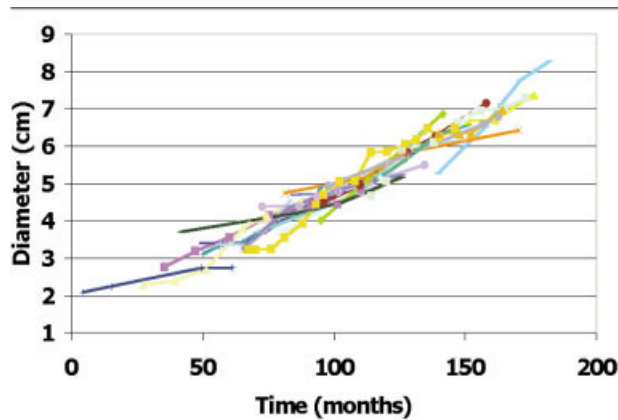


Fig 3. Tumors diameter evolution after time adjustment. For each patient, the mean tumor diameter is plotted against his size-adjusted time. By eliminating the lead-time bias, this procedure shows that the evolution of mean tumor diameters is comparable among all of the patients.

continuously during their premalignant phase and do so at a relatively constant, and hence predictable rate.

Our intent was to focus on the natural history of the low-grade gliomas that may be followed up during several years before a treatment is needed,^{4,5} and our results therefore are valid only in this subset of patients before anaplastic transformation. Even in such a favorable group, evidence of relentless growth over time contrasts with the clinical impression that these tumors often stabilize for years before evidence of progression is identified. A probable explanation for this discrepancy is that a minor increase of tumor diameter is very difficult to identify by simple visual comparison of consecutive MRI without careful measurements, although these changes have important consequences in terms of tumor volume. For example, an increase of mean tumor diameter from 3 cm to 3.4 or 3.8 cm will lead to an increase of tumor volume of 45 and 100%, respectively.

Our data also indicate that the growth of the mean tumor diameter is apparently linear. According to the model developed by Swanson and colleagues,⁶ glioma growth does not obey an exponential evolution because many newly produced tumor cells diffuse into the surrounding parenchyma and their density does not reach the minimal threshold required to appear on MRI. In this situation, measuring the volumetric doubling time is not appropriate to describe the growth curves; rather, one can expect a linear evolution of mean diameter over time. Our results are compatible with this model.

Interestingly, despite the limitations of manual measurements and the large variation of mean tumor diameters at diagnosis, ranging from 2.1 to 7 cm, the curves of individual patients appear grossly parallel suggesting a common law of tumor growth. Indeed, a linear regression of diameter versus time using a mixed model shows that the average slope of the evolution of

mean diameter over time, β , is 0.00113cm/day ($\sigma = 0.00005$), corresponding to an increase of 4.1mm per year with a narrow CI (95% CI, 3.8–4.4mm/year).

Note again that this mean line of growth was obtained in untreated patients followed up for a minimal period of 2 years, excluding rapidly progressing patients who required earlier treatment, and ceased to be valid in case of anaplastic transformation. Our results are nevertheless relevant for a substantial group of low-grade oligodendrogliomas or mixed gliomas and indicates that the dynamic properties of these tumors are most often comparable between various patients. The underlying biological processes that determine tumor growth therefore should be similar, although still unknown.

Modeling radiological growth could be useful for the clinician. First, it would help to predict future MRI changes. Second, the observation that these tumors do not stabilize and that an important increase of tumor volume often is required to be easily detected in the clinical setting could support the authors who propose an early surgical approach when safe macroscopically complete resection is possible at the onset.^{7–9} Indeed, the “wait and see” policy^{10–12} often is based on the assumption that the tumor size may remain unchanged for prolonged periods. Third, patients whose evolution clearly differ from the mean line could be identified early, eventually leading to a “dynamic classification” of low-grade gliomas. Treatment guidelines then could be adapted accordingly. Finally, this model could be used to study the role of slowly acting or cytostatic treatment whose main effect would be to shift down the slopes of the growth curves.

We thank P. Broët for helpful discussions about statistical analysis and J. Hildebrand for his critical review of the manuscript.

References

1. WHO Classification of Tumours. Pathology and genetics. Tumours of the nervous system. Kleihues P, Cavenee WB, eds. Lyon: IARC Press, 2000.
2. Woodward DE, Cook J, Tracqui P, et al. A mathematical model of glioma growth: the effect of extent of surgical resection. *Cell Prolif* 1996;29:269–288.
3. Swanson KR, Alvord Jr EC, Murray JD. A quantitative model for differential motility of gliomas in grey and white matter. *Cell Prolif* 2000;33:317–329.
4. Celli P, Nofrone I, Palma L, et al. Cerebral oligodendroglioma: prognostic factors and life history. *Neurosurgery* 1994;35:1018–1034; discussion, 1034–1035.
5. Piepmeyer J, Christopher S, Spencer D, et al. Variations in the natural history and survival of patients with supratentorial low-grade astrocytomas. *Neurosurgery* 1996;38:872–878; discussion, 878–879.
6. Swanson KR, Alvord Jr EC, Murray JD. Virtual brain tumors (gliomas) enhance the reality of medical imaging and highlights inadequacies of current therapy. *Br J Cancer* 2002;86:14–18.
7. Berger MS, Deliganis AV, Dobbins J, et al. The effect of extent of resection on recurrence in patients with low grade cerebral hemisphere gliomas. *Cancer* 1994;74:1784–1791.

8. Scerrati M, Roselli R, Iacoangeli M, et al. Prognostic factors in low grade (WHO grade II) gliomas of the cerebral hemispheres: the role of surgery. *J Neurol Neurosurg Psychiatry* 1996;61:291–296.
9. Keles GE, Lamborn KR, Berger MS. Low-grade hemispheric gliomas in adults: a critical review of extent of resection as a factor influencing outcome. *J Neurosurg* 2001;95:735–745.
10. Recht LD, Lew R, Smith TW. Suspected low-grade glioma: is deferring treatment safe?. *Ann Neurol* 1992;31:431–436.
11. Cairncross JG. Understanding low-grade glioma: a decade of progress. *Neurology* 2000;54:1402–1403.
12. Olson JD, Riedel E, DeAngelis LM. Long-term outcome of low-grade oligodendroglioma and mixed glioma. *Neurology* 2000;54:1442–1448.

Diminished Striatal [¹²³I]Iodobenzovesamicol Binding in Idiopathic Cervical Dystonia

Roger L. Albin, MD,^{1,2} Donna Cross, BSE,^{3,4} Wayne T. Cornblath, MD,^{2,5} John A. Wald, MD,² Kristine Wernette, MSN,^{2,6} Kirk A. Frey, MD, PhD,^{2,6} and Satoshi Minoshima, MD, PhD⁴

Striatal dysfunction is thought to underlie many dystonias. We used [¹²³I]iodobenzovesamicol single-photon emission computed tomography imaging to determine the density of cholinergic terminals in the striatum and other brain regions in 13 subjects with idiopathic cervical dystonia. Striatal [¹³¹I]iodobenzovesamicol binding was reduced. These results support a role for striatal dysfunction in idiopathic dystonias and suggest diminished striatal cholinergic interneuron density in cervical dystonia.

Ann Neurol 2003;53:528–532

From the ¹Geriatrics Research, Education, and Clinical Center, Ann Arbor VAMC; ²Department of Neurology and ³Neuroscience Graduate Program, University of Michigan, Ann Arbor; ⁴Department of Radiology, University of Washington, Seattle; and Departments of ⁵Ophthalmology and ⁶Radiology, University of Michigan, Ann Arbor, MI.

Received Sep 6, 2002, and in revised form Dec 13. Accepted for publication Dec 16, 2002.

Published online Mar 24, 2003, in Wiley InterScience (www.interscience.wiley.com). DOI: 10.1002/ana.10527

Address correspondence to Dr Albin, Neuroscience Laboratory Building, 4412D Kresge III, 200 Zina Pitcher Place, Ann Arbor, MI 48109-0585.

E-mail: ralbin@umich.edu

This article is a US Government work and, as such, is in the public domain in the United States of America.

Dystonias are a class of involuntary movements characterized by sustained postures of affected muscle groups, often with a torsional or rotatory component. Dystonia may be secondary to an identifiable pathological process involving the nervous system or idiopathic. The pathophysiology of dystonia is unknown. Pathological examination of primary dystonias has been unrevealing.¹ In secondary dystonias due to focal brain lesions, the putamen is the most common site of brain injury, though thalamic and brainstem lesions are associated also with dystonia.^{2–5} The loci responsible for some forms of inherited generalized dystonia are known. Dominantly inherited dopa-responsive dystonia (DRD; DYT5; Segawa's syndrome) is caused by mutations in GTP cyclohydrolase I, the rate limiting enzyme in synthesis of tetrahydrobiopterin, a necessary cofactor for tyrosine hydroxylase activity.⁶ Recessive DRD is associated with mutations in tyrosine hydroxylase itself.⁶ The more common childhood or adolescent-onset idiopathic torsion dystonia (ITD; DYT1), a dominantly inherited disorder with incomplete penetrance, is caused by mutations in the *torsinA* gene, a probable ATPase chaperone protein, which is expressed at high levels in substantia nigra dopaminergic neurons.⁶ The association of putamenal injury with secondary dystonia and the existence of dopamine synthesis abnormalities in DRD indicate that abnormalities of basal ganglia function underlie some forms of dystonia and lead to the suggestion that most forms of dystonia result from basal ganglia dysfunction. Perlmutter's group published imaging data consistent with putamenal abnormalities in idiopathic dystonia.^{7,8}

Some evidence suggests that dystonia results from abnormal sensorimotor coordination at the level of the neocortex as a downstream effect of striatal dysfunction (reviewed in Tamburin and colleagues).^{1,9} Some functional imaging evidence indicates abnormal sensorimotor processing in dystonias.^{10,11} Striatal cholinergic interneurons are suggested to mediate some forms of sensorimotor integration, raising the possibility that striatal cholinergic interneuron abnormalities could underlie dystonia.¹² We evaluated this possibility with [¹²³I]iodobenzovesamicol (IBVM) single-photon emission computed tomography (SPECT) imaging, a method that gives an estimate of the density of cholinergic nerve terminals.

Subjects and Methods

Subjects

Thirteen subjects with idiopathic cervical dystonia were recruited from the Botulinum Toxin Clinic at the University of Michigan. The mean age was 53 years (range, 41–71 years). There were 10 female subjects and 3 male subjects. The mean duration of cervical dystonia was 7.3 years (range, 1–21 years). Two subjects had associated blepharospasm and one had associated oromandibular dystonia. Two subjects